Slow dynamics in the geometrically frustrated magnet $ZnFe_2O_4$: Universal features of aging phenomena in spin glasses

H. Mamiya, N. Tsujii, N. Terada, S. Nimori, and H. Kitazawa
National Institute for Materials Science, Tsukuba 305-0047, Japan

A. Hoshikawa and T. Ishigaki
Ibaraki University, Tokai 319-1100, Japan

(Received 18 April 2014; revised manuscript received 14 July 2014; published 31 July 2014)

To clarify the universal features of spin glasses, we carefully studied slow dynamics in a geometrically frustrated magnet $ZnFe_2O_4$ with slight disorders, regarded as an "unconventional" Heisenberg spin glass, using time-resolved neutron diffractometry and magnetometry. The results indicate that "aging" can be attributed not to growth of the short-range order detected by a diffuse scattering but to aging of a hidden aperiodic correlation, as expected from theories for spin glasses. Concerning aging, peculiar behavior was found; the decay of thermoremanent magnetization is extremely accelerated if the sample is heated/cooled briefly midway through the isothermal slow relaxation. Conversely, magnetization surprisingly increases despite the absence of a magnetic field when the temperature returns after the brief heating/cooling. The behavior can be explained as a destabilization of the aged spin configuration due to the thermal perturbations and subsequent spontaneous restoration of the original spin configuration after the destabilization. Whereas such destabilization and restoration do not occur during freezing into numerous metastable states in a fixed energy landscape, these are possible in an energy landscape with a temperature-sensitive funnel-like structure. These features, consistent with the ghost domain scenario of the droplet picture, are the same as for conventional Heisenberg spin glasses such as dilute magnetic alloys and dilute magnetic semiconductors. In other words, they are universal features in Heisenberg spin glasses including unconventional ones.

DOI: 10.1103/PhysRevB.90.014440 PACS number(s): 75.50.Lk, 75.10.Nr, 75.40.Gb

I. INTRODUCTION

Glassy systems are ubiquitous in daily life; however, little is known regarding their nature. An example is spin glass, one of the most theoretically studied glassy systems, where the theories predicting aperiodic long-range ordered states have been little verified by experiments [1–3]. The reasons are simple. Briefly, this kind of ordering needs geological time scales to form; hence, the long-range fully ordered spin structure in the equilibrium state cannot be observed, if it ultimately does exist, in any experiment. Furthermore, diffractometry, a decisive technique for conventional spin structures, is not helpful in studying such aperiodic order. Indeed, various diffuse scatterings have been observed in some spin glasses [4,5], while profiles of the diffuse scatterings do not change across the spin-glass transition temperature T_g. Thus, the relationship between the scatterings and spin glass is still unclear. In this stage we are interested in which kinds of measurable properties characterize the spin glass state, because neither the lack of magnetic Bragg peaks below T_g nor the absence of anomalies in specific heats at T_g are suitable when comparing observations and theoretical predictions in detail [1]. Magnetohistory effects such as differences between the zero-field-cooled and field-cooled magnetization and extremely slow dynamics were frequently observed in spin glasses [1–3], but these behaviors have also been reported in periodically ordered magnets [6–8]. In this context, aging, rejuvenation, and memory effects observed in nonequilibrium phenomena were considered key in clarifying the nature of spin glass [3,9–15] because the three effects were reported together only in materials regarded as spin glass. Recently, using original protocols, these characteristic effects have been re-examined in conventional Heisenberg spin glasses such as dilute magnetic alloys and semiconductors [16–19]. Consequently, the obtained results demonstrate an energy landscape with a temperature-sensitive funnel-like structure. This feature well fits the ghost domain scenario [13] among the models proposed in the long-standing controversy. For this reason, universality in nonequilibrium phenomena of spin glasses including unconventional ones now attracts much attention.

In geometrically frustrated magnets, spin-glasslike behavior as well as spin-ice and spin-liquid properties has been repeatedly reported [20–25], where no long-range magnetic orders have been observed, although the density of the interacting spins is much higher than the percolation limit. A noteworthy point is that the aging, rejuvenation, and memory effects coexist in some frustrated magnets such as pyrochlore-type $Y_2Mo_2O_7$ [26] and cubic spinel-type $ZnFe_2O_4$ [27]. At the present time, it is uncertain whether the conditions associated with these spin-glasslike properties include a degree of randomness as well as frustration, because we cannot prepare perfect single crystals without structural or chemical defects. Apart from this tough issue, the actual frustrated magnets exhibiting these properties have been known as "unconventional" or "topological" spin glasses [23,24]. For this reason, detailed investigation of their nonequilibrium phenomena is valuable for clarifying the universal nature of spin glass. In this study, we chose $ZnFe_2O_4$ from among these frustrated magnets, because its spin is rather large ($S = 5/2$) and well localized on one magnetic lattice. Additionally, it has no-orbital degree of freedom [$(t_{2g})^5$]. For this simple classical Heisenberg system, we carefully studied nonequilibrium phenomena by time-resolved neutron

TABLE I. Refined structural parameters of $ZnFe_2O_4$ at room temperature, where a is the lattice constant and U_{iso} is the isotropic displacement parameter. We also refined the occupancies of zinc and iron ions in the 8a and 16d sites. The R factors in Rietveld analysis are R_{wp} of 0.044, R_p of 0.036, and R_e of 0.028.

a (nm)	Site	Occupancy	x	y	z	U_{iso} (pm^2)
0.844282(1)	8a	Zn: 0.893(2) Fe: 0.107(2)	0	0	0	49.6(5)
	16d	Zn: 0.054(1) Fe: 0.946(1)	0.625	0.625	0.625	45.8(3)
	32e	O: 1.0	0.38488(1)	0.38488(1)	0.38488(1)	56.6(3)

diffractometry and magnetometry, because scattered neutrons or linear responses to sufficiently weak magnetic fields provide measures that mirror the dynamics of the spin configuration on different observation times without effects on the intrinsic evolution of the spin configuration.

II. SAMPLE AND EXPERIMENTS

Sintered powder of the zinc-ferrite $ZnFe_2O_4$ was prepared using a standard solid-state reaction. Appropriate ratios of ZnO (99.9% purity) were mixed with Fe_2O_3 (99.99%) and then pressed into pellets. The pellets were annealed in air at 1523 K for 24 h, and finally quenched in liquid nitrogen. The ratio of Zn ions to Fe ions determined by inductively coupled plasma optical emission spectrometry was 0.50. The crystal structure of this sample was characterized using a high throughput neutron powder diffractometer (iMATERIA) at the Japanese particle accelerator research complex (J-PARC). Rietveld refinements were performed for the diffraction pattern at room temperature using the program Z-Rietveld. The results indicate that the sample was made of a single cubic spinel phase; the refined parameters are shown in Table I. The occupancy of nonmagnetic Zn ions in the 16d site was estimated to be 0.054. Note that it matters little whether the geometrical frustration in this sample is far from perfect as our concern here is the features of "unconventional" spin glass observed in an actual frustrated magnet with inevitable disorders.

Low-temperature elastic neutron powder diffractions were measured for a 5.0-g powder packed in a vanadium can under helium gas, using high-resolution detector bank and low-angle detector bank equipped in iMATERIA, where the temperature was controlled in the range from 10 to 50 K using a closed cycle refrigerator. Time-resolved neutron diffraction measurements started instantly after the sample was quenched ($t = 0$) from 50 K to the desired temperature $T_0 = 15.2$ K. At $t_1 = 11$ ks, the sample was temporarily cooled to $T_0 - |\Delta T| = 13.5$ K and then reheated to T_0 at $t_2 = 22$ ks. This experiment was performed in a zero magnetic field.

The magnetization and the ac susceptibility $\chi' + i\chi''$ were measured on a sintered chip of 24 mg weight using a SQUID magnetometer, where the constant magnetic field H of 297 A/m in the linear response regime or the alternating field $h_{ac}\cos(2\pi f \cdot t)$ with h_{ac} of 297 A/m and f of 800 mHz was generated by a normal conducting coil in a Permalloy magnetic shield, giving a residual field below 1 A/m. Concerning their temperature dependence, the zero-field-cooled magnetization M_{ZFC} was measured on a heating process in H after zero-field cooling; the field-cooled magnetization M_{FC} was recorded on a cooling process in H; the thermoremanent magnetization M_{TRM} was measured during a heating process in $H = 0$ after the field-cooling process. These cooling/heating cycles were made in the range between 50 and 5 K, where the sweep rate during the measurements was 17 mK s^{-1}. The ac susceptibility was measured while heating from 6 K in a zero static field at a sweep rate of 2 mK s^{-1}.

As for the study on relaxation of thermoremanent magnetization M_{TRM}, the sample was isothermally pre-equilibrated for waiting time t_w after being quenched to $T_0 = 15.0$ K in a magnetic field H. Then, the measurement of M_{TRM} was started just after H is removed at $t = 0$. In contrast, the recording of χ'' began immediately after the sample was quenched ($t = 0$) from 50 K to $T_0 = 15.0$ K in a zero magnetic field. In one case, the sample was temporarily cooled to $T_0 - |\Delta T| = 13.5$ K at $t_1 = 6.3$ ks and then reheated to T_0 at $t_2 = 12.8$ ks, whereas in another the recording was isothermally continuous, the data being used in providing reference curves. In addition to these experiments using the standard protocols for spin glass [2,3], we employed the following original thermal history: The sample was temporarily heated/cooled to $T_0 \pm |\Delta T|$ at $t_1 > 0$ and then recooled/reheated at $t_2 > t_1 > 0$ halfway through the decay of M_{TRM}. Similarly, we recorded the behavior of M_{ZFC} for the same temporary heating/cooling from t_1 to t_2, with the probe field H applied at $t = 0$ after isothermal pre-equilibration for t_w in a zero magnetic field.

III. RESULTS

A. Neutron scattering

Figure 1 shows the neutron diffraction patterns obtained at various temperatures between 10 K and room temperature. Noticeable diffuse scattering can be found around a scattering vector $q = 6$ nm^{-1}, whereas in the q range from 10 to 50 nm^{-1} there are no evident differences between the patterns at low temperatures and that at room temperature. As shown in the inset, the position of the diffuse scattering shifts toward lower q and its intensity gradually decreases with increasing the temperature from 10 K. These properties are consistent with the prior report [28,29] where it has been experimentally observed that the diffuse scattering appears around the same q value, but never rises to the level of the magnetic Bragg peak even when the sample is cooled to very low temperatures. In a recent study using a single crystal, the short-range correlation causing this diffuse scattering has been interpreted as spin molecules of a kagome-star dodecamer [30]. There is, however, room for further investigation. For example, thermal stability of the dodecamer is still unclear, hence, no explanation

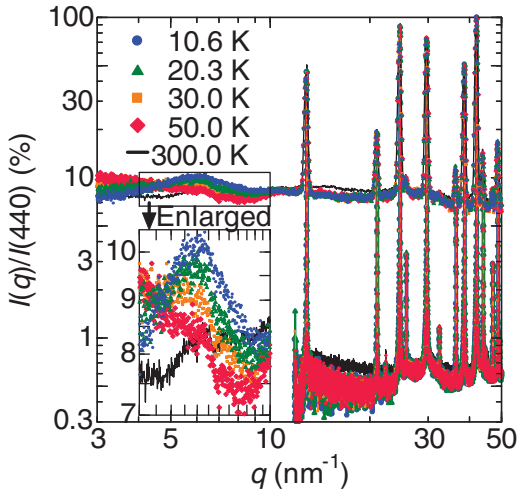

FIG. 1. (Color online) Neutron powder diffraction patterns at various temperatures, where q is the scattering vector and the intensity is normalized by the maximum value at reflection from the (440) plane. The uppermost patterns were obtained by the low-angle detector bank and the lowermost by the high-resolution detector bank. The patterns around $q = 6$ nm^{-1} are enlarged in the inset.

has been established for the temperature dependence of diffuse scattering profile.

Figure 2 shows the time variation of the diffuse scattering on the isothermal waiting and the subsequent thermal perturbation. There is no evident difference between the profiles except for a slight difference between the locations of the peak at the two different temperatures (see arrows in Fig. 2). The full-width at half-maximum (FWHM) obtained

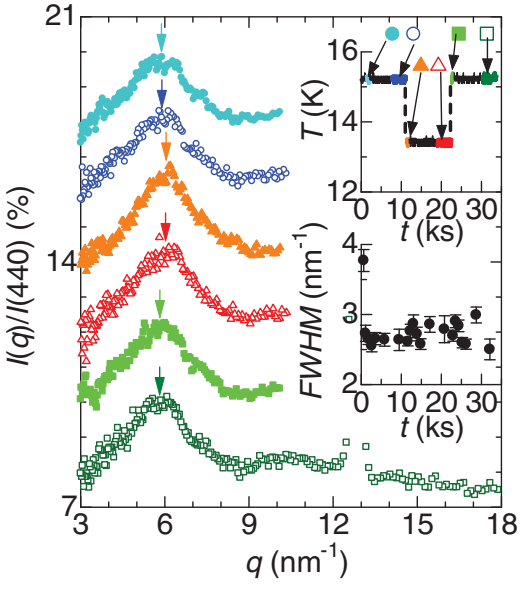

FIG. 2. (Color online) Evolution of diffuse scattering on the thermal history shown in the upper inset, where base lines have been shifted for greater clarity. The arrows mark the scattering vector q when the intensity becomes maximum. The lower inset shows evolution of the full-width at half-maximum (FWHM) obtained by assuming a Lorentz profile for the diffuse scattering peaks.

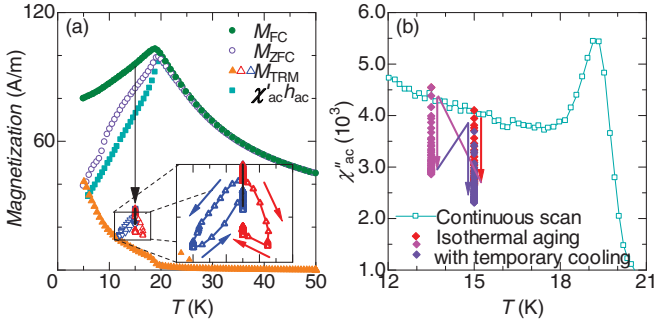

FIG. 3. (Color online) Temperature dependence of various magnetic responses. Solid and open circles and solid triangles in (a), respectively, indicate the conventionally observed zero-field-cooled magnetization $M_{\rm ZFC}$, field-cooled one $M_{\rm FC}$, and thermoremanent one $M_{\rm TRM}$ for an applied field H of 239 A/m and a sweep rate of 17 mK s^{-1}. The solid squares in (a) and the open squares in (b), respectively, show the in-phase and out-of-phase components of the ac susceptibility χ' and χ'' at amplitude $h_{\rm ac} = 239$ A/m and frequency $f = 800$ mHz. The open triangles in (a) represent the variations of $M_{\rm TRM}$ on the positive/negative thermal cycling shown in the insets in Figs. 6 and 8, while the solid diamonds in (b) denote the variations of χ'' on the thermal cycling shown in the inset in Fig. 5. (Note: The time evolutions of $M_{\rm TRM}$ and χ'' on the same thermal cycling are shown in Figs. 5, 6, and 7 using the same symbols.)

assuming a Lorentz profile seems almost constant during the experiments, as shown in the inset. (The exception is the first data obtained just after initial quench from 50 K, where temperature inhomogeneity may still exist in the large quantity of powder used for neutron diffractometry.)

B. Magnetic response obtained by the standard protocols for spin glass

Figure 3(a) shows the temperature dependence of $M_{\rm ZFC}$, $M_{\rm FC}$, $M_{\rm TRM}$, and $\chi' h_{\rm ac}$. We see that, at higher temperatures, $M_{\rm ZFC}$, $M_{\rm FC}$, and $\chi' h_{\rm ac}$ are the same and gradually increase as temperature is lowered. At $T_{\rm g} \sim 20$ K, they show a cusp. Below $T_{\rm g}$, $M_{\rm ZFC}$ noticeably deviates from $M_{\rm FC}$ and $\chi' h_{\rm ac}$ also drops with decreasing temperature. In this temperature range, $M_{\rm TRM}$ remains nonzero. This result indicates that the magnetic response markedly slows down below $T_{\rm g}$, and consequently magnetohistory effects appear over the temperature range. These properties are common to conventional spin glasses, although the decrease in $M_{\rm FC}$ with decreasing temperatures below $T_{\rm g}$ seems steeper than the spin glasses [31,32]. In contrast, for the temperature dependence of χ'' [Fig. 3(b)], we find a cusp at a temperature slightly lower than $T_{\rm g}$ and a gently sloping plateau in the lower temperature range. This property is essentially the same as for conventional spin glasses (see p. 21 in [2]).

The solid lines in Fig. 4 mark the isothermal relaxation curves for thermoremanent magnetization $M_{\rm TRM}$, plotted on a logarithmic time scale. As anticipated above, $M_{\rm TRM}$ gradually decreases in a zero magnetic field. As the period $t_{\rm w}$ increases, this decay in $M_{\rm TRM}$ slows down. This figure indicates that the maximum decay rate $-\Delta M_{\rm TRM}/\Delta \ln t$ appears at an observation time close to $t_{\rm w}$ (marked by arrows in Fig. 4). This behavior, known as aging, has been generally explained

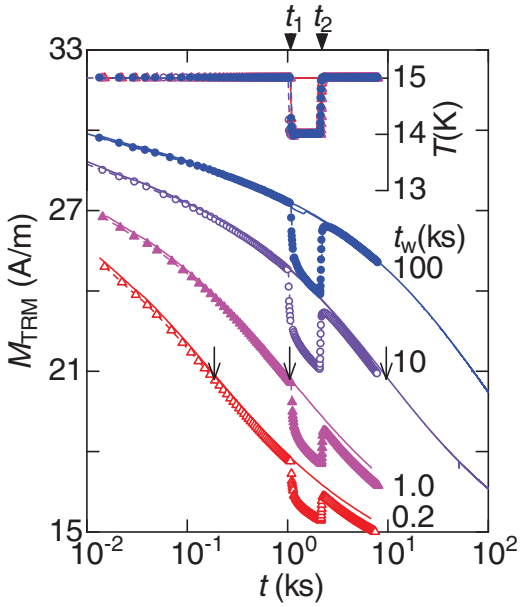

FIG. 4. (Color online) Decay curves of thermoremanent magnetization M_{TRM}. After quenching in magnetic field $H = 297$ A/m, the system was maintained at $T_0 = 15.0$ K for an isothermal waiting period t_w; then, the magnetic field was removed at T_0 and $t = 0$. In some cases, at $t_1 = 1.1$ ks the system was temporarily cooled to $T_0 - |\Delta T| = 14.0$ K, and then reheated at $t_2 = 2.2$ ks, as indicated in the inset. The solid curves represent the isothermal reference curves and the symbols show the variations with temporary cooling. The arrows mark the time when isothermal decay rate $-\Delta M_{TRM}/\Delta \ln t$ becomes maximum.

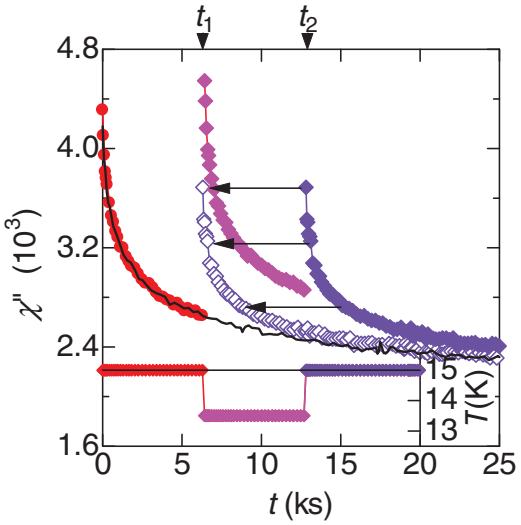

FIG. 5. (Color online) Evolution of the out-of-phase component of ac susceptibility χ'', where an alternating field at amplitude $h_{ac} = 239$ A/m and frequency $f = 800$ mHz was continuously applied after initial quench from 50 K at $t = 0$. The solid diamonds show χ'' upon temporary cooling from t_1 to t_2, whereas the solid line represents the isothermal variation of χ'' (reference curve.) The open diamonds indicate that the χ'' shifted leftward by $t_2 - t_1 = 6.5$ ks (see the arrows.) The inset shows the thermal history of the measurements.

as a kind of stabilization of the spin configuration during the aging period t_w leads to a delay of the magnetic response by approximately t_w [2,3].

Figure 5 shows the time variation of the loss-component χ'' of the ac susceptibility. We can see that χ'' gradually decreases with time after quenching. The decrease continues even after a few hours have passed. This isothermal decrease has been attributed to the system becoming less dissipative with a kind of ordering of the spin configuration. In other words, this is also an aging phenomenon. The remarkable point is that when the system is further cooled to $T_0 - |\Delta T| = 13.5$ K at t_1, it recovers its high dissipative nature, as if rejuvenated to the initially observed state at $t = 0$. This "rejuvenation" is also clearly seen in Fig. 3(b) where the temperature dependence of the same χ'' as Fig. 5 is shown. After the temperature is stabilized at $T_0 - |\Delta T| = 13.5$ K, χ'' again decreases with time. One sees again that the system becomes dissipative when the temperature returns to $T_0 = 15$ K at t_2. Subsequently, χ'' steeply decreases with time and approaches the level that was observed just before thermal perturbations are applied. Here it is helpful to plot the same χ'' against time $t - (t_2 - t_1) = t - 6.5$ ks, as usually performed in studies on spin glasses (see open diamonds in Fig. 5) [2,3]. These open diamonds lie on the isothermal relaxation curve at $T_0 = 15$ K, except for the transient period for several kiloseconds after the temperature returns to its initial value. That is, the relaxation at $T_0 = 15$ K seems to continue across the thermal perturbation, despite the significant variation of χ'' during the thermal perturbation at $T_0 - |\Delta T| = 13.5$ K. This feature has been termed the "memory effect" [2,3]. Moreover, the observed transient period has been called "a recovery time of memory" [14], and the brief increase in χ'' in this period has been termed "a transient spike" [33] or "a transient faster relaxation" [10]. To sum up, the present experiments using the standard protocols for spin glass clearly show that aging, rejuvenation, and memory effects (also a transient spike) coexist in $ZnFe_2O_4$, as previously reported by a dip experiment [27].

C. Magnetic response obtained by the original protocols

Figures 4 and 6 show variations in M_{TRM} when temperature is temporarily cooled to $T_0 - |\Delta T|$ in the period from t_1 to t_2. The decay of M_{TRM} is found to accelerate at the onset of temporary cooling. The extent of acceleration becomes larger with increasing ΔT (see Fig. 6). In the framework of thermally activated dynamics, no explanation is possible for this accelerated relaxation resulting from cooling. At the end of temporary cooling, more surprising results are observed: In a zero magnetic field, M_{TRM} values clearly increase if the system is reheated to $T_0 = 15$ K at t_2. By extending period t_w, M_{TRM} recovers to almost its original value just before the cooling period, as seen in Fig. 4.

Such unexpected acceleration and reversion of the decay were found by temporary heating (Figs. 7 and 8). For example, the decay rate increases approximately a hundredfold when the system is temporarily heated to $T_0 + |\Delta T| = 16.0$ K (see solid triangles in Fig. 8). We cannot easily interpret such extreme accelerations in decays by considering a simple activation dynamics because of the slightly enhanced thermal

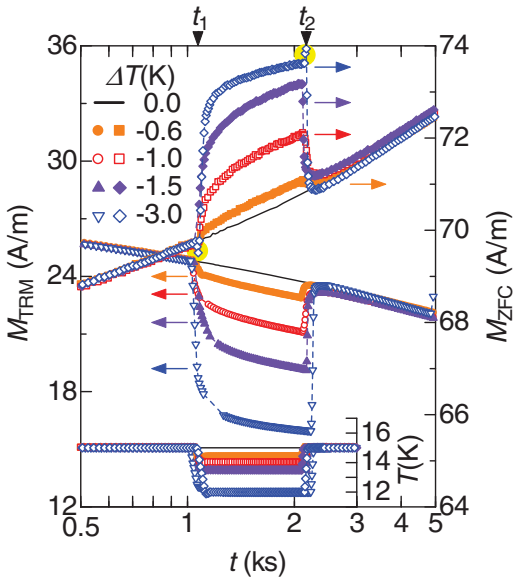

FIG. 6. (Color online) Relaxation curves of magnetization with temporary cooling periods at various ΔT. The sample was maintained at $T_0 = 15$ K during isothermal waiting periods of $t_w = 10$ ks in a constant (or zero magnetic field) after being quenched; then the recording of M_{TRM} (or M_{ZFC}) was started just after the field $H = 297$ A/m is removed (or applied) at $t = 0$. In some cases, at $t_1 = 1.1$ ks the sample was temporarily cooled to $T_0 + |\Delta T|$, and then reheated at $t_2 = 2.2$ ks, as indicated in the inset. The solid curves represent the isothermal reference curves and the symbols show the variations with the temporary cooling.

energies. Furthermore, a similar extraordinary increase in M_{TRM} in the zero magnetic field is also observed if the system is recooled after temporary heating, with period t_w sufficiently extended (see Fig. 7). In contrast, such an increase is not detected after a short t_w.

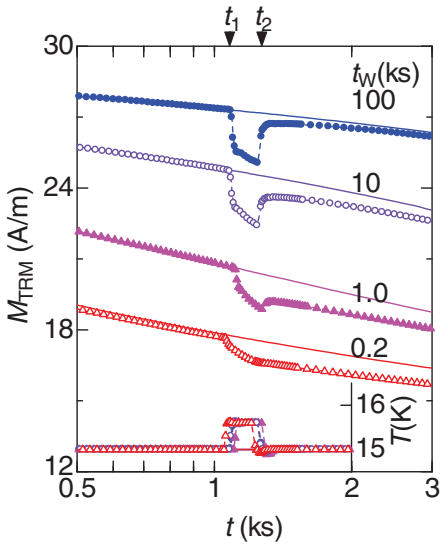

FIG. 7. (Color online) Same as for Fig. 4 except for temporary heating at $T_0 + |\Delta T| = 15.6$ K from $t_1 = 1.1$ ks to $t_2 = 1.3$ ks.

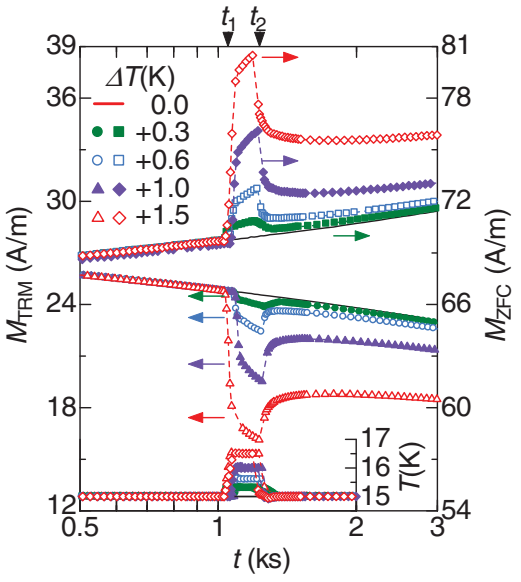

FIG. 8. (Color online) Same as for Fig. 6 except for temporary heating at $T_0 + |\Delta T|$ from $t_1 = 1.1$ ks to $t_2 = 1.3$ ks.

Figures 6 and 8 show the relaxation curves of the zero-field-cooled magnetization M_{ZFC} on the same positive/negative thermal perturbations after isothermal aging. The variations in M_{ZFC} on the onset and end of the perturbations are seen to proceed clearly towards opposite directions than those in M_{TRM}. The observed increase in M_{ZFC} on cooling and its decrease on reheating may be explained by the coexistence of the paramagnetic secondary phase; however, the opposite variations in M_{TRM} cannot be interpreted in the same manner (see Fig. 6). Furthermore, the observed decrease in M_{TRM} on heating and increase on recooling (see Fig. 8) are reasonable if the effective magnetic moment contracts with increasing temperature; however, the variations in M_{ZFC} are impossible with this assumption. As exemplified here, no models assuming a kind of thermally reversible component can satisfy both the extraordinary variations in M_{TRM} and M_{ZFC}. In other words, we can conclude that they are accelerations and reversals associated with magnetic relaxations. This conclusion is supported by the fact that they are symmetrical with respect to positive/negative thermal perturbations. The intriguing nature associated with these phenomena will be discussed next.

IV. DISCUSSION

A. Magnetic short-range order and existence of hidden magnetic ordering process

First of all, we shall begin the discussion by reconsidering whether there is any classical long-range order for spins, for we now know that a kind of ordering in the spin configuration gradually proceeds after cooling. That is, we must examine the possibility that the observed diffuse scattering profile is merely a snapshot and narrows slowly. The key issue is the isothermal evolution of the dissipative property. Note that boundaries must exist if the system is divided into short-range ordered regions. Generally speaking, the dissipation from the excitations inside

the ordered regions is stationary, while the boundaries are unstable and highly dissipative. Therefore, a decrease in dissipation should be attributed to variations of the boundaries; i.e., disappearance of the boundaries due to the growth of the ordered regions. Assuming compact ordered regions, the total area of the boundaries per unit volume is inversely proportional to the correlation length. That is, the reduction in χ'' by half means a doubling of the correlation length when the stationary part is negligible. Actually, the increase in correlation length should be greater because of the stationary part. For this reason it is reasonable to expect significant growth of the correlated regions based on the reduction shown in Fig. 5, although the model used here may be oversimplified. In contrast to this expectation, the FWHM of the diffuse scattering peak, which is inversely proportional to the correlation length, seems almost constant during the isothermal aging period. Apart from the initial period of ambiguity in temperature, the variation of FWHM in the period from $t = 1$ to 10 ks is smaller than 10%, while the correlation length is expected to extend by more than 30% in the same period. In other words, the stabilization of the spin configuration is difficult to explain as a growth in the observed short-range order. This fact is consistent with the experimental results that there is no sudden change in the diffuse scattering profile across $T_g \sim 20$ K; χ' shows a cusp. There is no need to go into details about the stable short-range order, although it is open to question as stated above. The reason is that our concern is on slow dynamics.

Let us address the question what kind of ordering stabilizes the spin configuration without changing the neutron scattering profile. A plausible origin is the evolution of an aperiodic correlation which is difficult to observe using diffractometry. This hypothesis is supported by the observed slow dynamics as extremely slow relaxations have long been known to occur in glassy systems. This reasoning leads on to querying the nature of the aperiodic correlation. Is it related to the observed short-range order? It is helpful to recall that a stringlike medium-range ordering has been considered between icosahedral clusters in metallic glasses [34] and that the randomly oriented interparticle correlation has been discussed between ferromagnetically short-range-ordered nanoparticles in superspin glasses [31]. In this context, an aperiodic superstructure could exist between the above-mentioned spin molecules, where the slow evolution of χ'' can be attributed to the growth of the superstructure, whereas the fast fluctuations observed inelastic neutron scattering [30] correspond to excitation in the spin molecules. This concept resembles α and β relaxations in structural glasses. Nevertheless, we must bear in mind the other possibility that spin-glasslike correlated regions coexists with the spin molecules as an inhomogeneous system [35]. At this stage, the issue remains open because there is no experimental method to locally distinguish aperiodic correlations from short-range order.

We return to the main theme, whether the properties of $ZnFe_2O_4$, termed "unconventional" spin glasses, have common features with other spin glasses. The immediate answer is that the slow dynamics seems related with evolution of a hidden aperiodic correlation, as for conventional Heisenberg spin glasses [36]. Nevertheless, the stationary diffuse scattering due to kagome-star dodecamers can be considered specific to $ZnFe_2O_4$. To clarify the universality further, details of the macroscopically observed slow dynamics, caused by the slow evolution of a hidden aperiodic correlation, are discussed next.

B. A rugged energy landscape of the spin configuration space

In ideal geometrically frustrated magnets, the ground state is highly degenerate; however, it has been argued that the low level of disorder that generally exists in actual materials lifts the degeneracy [20,37]. The large number of possible configurations leads to a large number of states with similar energy but separated by barriers with various heights; this forms a rugged energy landscape with numerous valleys in the spin configuration space. In this landscape we can expect thermally activated explorations for deeper valleys after quenching from a paramagnetic state. For simplicity we currently classify the barriers as high, moderate, and low with respect to thermal energy $k_B T_0$; the first are almost impenetrable, the second requires substantial time for jumps to occur, and the third can be surmounted instantly. If the number of lower barriers is larger, the landscape is a typical valley-in-valley structure: shallow valleys separated by low barriers coexist in low areas which are surrounded by the moderate barriers that in turn form the fine structure of the landscape formed by the high barriers. Therefore, we observe jumps over the moderate barriers as slow isothermal aging, whereas values corresponding to the probability of being in the shallow valleys immediately equilibrate across those areas surrounded by the moderate barriers. The landscape of the energy surface is sketched in Fig. 9(a). When the explored valleys become deeper (or the barriers become higher) with the jumps, the dissipation lessens; consequently, the loss-component χ'' declines as seen in Fig. 5. The observed delay of the magnetic response by t_w is explained as follows: Time for escaping from the valley over the surrounding barriers is comparable with the time for jumping into the valley.

Next, we shall discuss the evolution during temporary cooling, where the energy landscape at $T_0 - |\Delta T|$ is assumed to be the same as at T_0 (fixed landscape picture [12]). When temperature is lowered, even the moderate barriers become insurmountable. This leads to confinement of the system in those areas surrounded by moderate barriers. However, the configuration is neither frozen nor stable, because Boltzmann weights for the probability of being in the shallow valleys change with temperature. This instability leads to enhancement of the dissipation, i.e., rejuvenation at the beginning of the cooling period, as shown in Fig. 5. The subsequent slow reduction of χ'' in the cooling period can be explained as a local equilibration of the unequal probabilities of being inside the confinement area [note arrows in the lower panel of Fig. 9(a)]. When the temperature returns to T_0, the Boltzmann weights return to their original values. Consequently, the system becomes transiently dissipative again. Local equilibration again occurs inside the confinement area. Note that the status of the spin configuration after this equilibration should be the same as just before temporary cooling. With the exception for the transient period, this is a possible reason why the open diamonds in Fig. 5 lie on the isothermal relaxation curve at $T_0 = 15$ K. To sum up, the change in Boltzmann

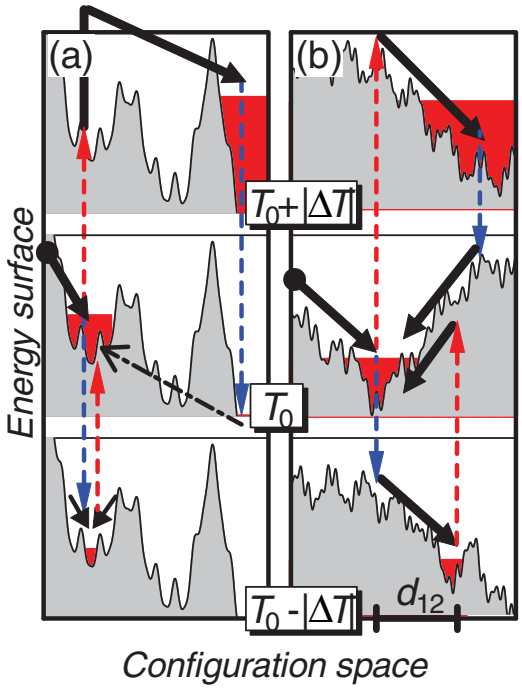

FIG. 9. (Color online) Rough sketches of the landscape of the energy surface in the spin configuration space at three slightly different temperatures, $T_0 + |\Delta T|$ (lower panels), T_0 (center panels), and $T_0 + |\Delta T|$ (upper panels): (a) a multi-deep-valley structure and (b) a temperature-sensitive funnel-like structure. The thick arrows, starting from the solid circles, denote possible evolutions during aging at the temperatures, whereas the broken arrows indicate variation during heating and cooling. The alternate long and short dash arrow in (a) represents an impossible evolution.

weights induced by thermal perturbations certainly causes the transient increases at the beginning and end of the temporary cooling period, whereas the confinement during cooling leads to a memory effect. As described here, the experimental results obtained by the standard protocols can be qualitatively explained using the fixed energy landscape picture for the spin configuration space. In real space, a similar interpretation would be possible by considering randomly pinned domain walls, where the depths of the pinning potentials are also random.

However, this picture has difficulty in explaining the experimental results obtained by the original protocols. For example, from the behavior in Figs. 4 and 6, the drop in M_{TRM} during the cooling period and the increase in M_{TRM} after reheating can be explained by assuming that the magnetization of the locally equilibrated state inside the confinement area decreases with lowering temperature. However, this explanation cannot be applied to the equivalent variations induced by the temporary heating (see M_{TRM} in Figs. 7 and 8). As an alternative explanation of these variations, we can consider that higher thermal excitations during heating enable escapes from the confinement area; consequently, the configuration stochastically reaches more stable states with lower magnetization [note arrows in the upper panel of Fig. 9(a)]. This leads to a decrease in M_{TRM} in the temporary heating period. In this case, M_{TRM} increases after re-cooling should be explained as a spontaneous return to the original valley: the alternate long and short dash arrow in Fig. 9(a). Unfortunately, there is no mechanism for such spontaneous returns because, in a zero magnetic field, the original valley with higher magnetization is not the most stable among the numerous neighboring valleys. As exemplified here, the changes in Boltzmann weights are insufficient to be able to account for all the results in Figs. 4, 6, 7, and 8 simultaneously. For this reason, we must modify the structure of the energy landscape in the spin configuration space.

C. Temperature sensitive funnel-like structure of the energy landscape

One feasible modification is that the landscape dramatically changes with temperature. Barrier disappearances caused by thermal perturbations lead to accelerated magnetic relaxation until higher barriers generated at other locations at the new temperature are encountered [note arrows in the lower panel of Fig. 9(b)]. It is interesting to consider how long the system takes to explore the region during this period. In Fig. 6 the magnitude of the decrease in M_{TRM} by thermal perturbation at $\Delta T = -3$ K is approximately one-third of the initial value just after switching off H. If the system is assumed to have been homogeneously magnetized in its initial state, then one-sixth of the spins are possibly flipped. In the spin-configuration space, the transfer distance during cooling, $d_{12} = (4N)^{-1}\Sigma[S_i(t_1) - S_i(t_2)]^2$, is given as $q_{\mathrm{EA}}/6$, where N is the number of spins, S_i denotes the spin at site i, and q_{EA} is the self-overlap or the so-called Edwards-Anderson order parameter. The homogeneity assumption is arguable, as discussed above; hence this estimation must be examined from other perspectives. For this purpose we recall the above rough argument that the correlation length is inversely proportional to the magnitude of χ''. Following this argument, the observed steep reduction of χ'' in the temporary cooling period indicates a significant growth of the hidden correlation. Because such a growth is accompanied with major rearrangements of the spin configuration, we can say the transfer distance during accelerated explorations d_{12} is not negligible in comparison with the scale of the configuration space.

Next, we shall reconsider M_{TRM} increases in a zero magnetic field. As discussed above, this extraordinary behavior is attributed to the reversal of the magnetic relaxation. In the energy landscape, the behavior is regarded as a spontaneous return to the original valley at the ends of thermal perturbations. Such a return cannot occur if other valleys with similar depths as the original are regenerated along the way. That is, the basin of attraction corresponding to the original valley covers the explored region of size d_{12}, although shallow valleys and barriers may appear on its energy surface. This indicates that the energy landscape is, at least in an observing range, not a multi-deep-valley structure but can be coarse grained as a funnel-like structure, as sketched in the center panel in Fig. 9(b). Considering the estimated long transfer distance from the original funnel existing at T_0 toward the funnel regenerated at $T_0 - |\Delta T|$, we can say that the locations of the funnels change critically with temperature in the spin configuration space.

In the ghost domain scenario of the droplet picture [13], an equilibrium state with a set of random bonds J_{ij} at temperature T is given by its stable spin configuration $\{\boldsymbol{S}_i^{(T,J)}\}$. The other possible stable configuration in the same environment (T, J_{ij}) is the only global spin inversion $\{-\boldsymbol{S}_i^{(T,J)}\}$. These configurations are paired like ferromagnets. That is, the number of global minima is only two in the spin-configuration space. Notable point of this picture is that $\{\boldsymbol{S}_i^{(T\pm|\Delta T|,J)}\}$ at different temperatures are entirely uncorrelated with $\{\boldsymbol{S}_i^{(T,J)}\}$ beyond an overlap length. In other words, the locations of the global minima change with temperature in a chaotic manner. These features well resemble those discussed above. Unfortunately, we cannot prove that the number of global minima is only two in the whole spin-configuration space because the explored region is limited. We can say that the width of each funnel, at least in one direction, is comparable with the scale of the configuration space.

The behavior observed in Fig. 5, the relaxation of χ'' is the continuation of the one that occurred before the temporary cooling, has been reported not only in spin glasses but also in re-entrant ferromagnets such as $CdCr_{1.8}In_{0.2}S_4$ [38], and in the stoichiometric ferroelectrics such as a single crystal of RbH_2PO_4 [39]. That is, the memory effect as to χ'' is not peculiar to spin glasses. A possible reason why this effect was observed in various systems is that the recovery of the dissipation χ'' after temporary cooling can also occur when a dissipation mechanism that is frozen at the lower temperatures is simply reactivated at the original temperature. Conversely, reversion of the relaxation of magnetization is attributed only to the spontaneous restoration of the original spin configuration. This behavior was known only in conventional Heisenberg spin glasses such as the dilute magnetic alloy $Cu_{97}Mn_3$ [16] and the dilute magnetic semiconductor $Cd_{55}Mn_{45}Te$ [19] so far. Therefore, we can conclude that the spontaneous restoration of the original spin configuration is, at least, a universal feature in Heisenberg spin glasses including "unconventional" spin glasses of the frustrated magnet $ZnFe_2O_4$, although it might be also observed in Ising spin glasses in the future.

V. SUMMARY AND PROSPECTIVE

To clarify the universal features of spin glasses, we carefully studied nonequilibrium phenomena of $ZnFe_2O_4$ with slight disorders, an "unconventional" Heisenberg spin glass, using time-resolved neutron diffractometry and magnetometry. Consequently, the slow dynamics can be attributed to the evolution of a hidden aperiodic correlation, as expected for spin glasses. Careful experiments using an original protocol showed not only a temporary accelerated decay in M_{TRM} at the beginning of positive/negative thermal perturbations but also a reversal of decay in a zero magnetic field at the end of the perturbations. They are attributed to destabilization of the aged aperiodic spin configuration and spontaneous restoration of the original spin configuration after rearrangement during the perturbations. In the energy landscape of the spin configuration space, a temperature-sensitive funnel-like structure was proposed to explain these extraordinary phenomena. The landscape features are consistent with predictions of the ghost domain scenario. This nature of the slow dynamics in $ZnFe_2O_4$ showed a common feature with conventional Heisenberg spin glasses.

The question as to what the hidden aperiodic correlation is remains open. Is it a super-spin-glasslike correlation between the spin molecules, or a kind of spin-glasslike second phase coexisting with the spin liquid phase of the spin molecules? As an initial response, any one of the spin-polarized (SP) transmission electron, SP-scanning electron, and SP-scanning tunneling microscopies at atomic resolutions may be helpful in studies. There would, however, remain room for further discussion even if all spin configurations were identified by these studies, because in principle one cannot distinguish in a finite experimental time aperiodic long-range ordered states with a randomly oriented spin configuration from states frozen from paramagnetic spin configurations. Therefore, we must develop further indirect approaches such as detailed comparisons of carefully observed aging phenomena with more accurate computer simulations enabled through dramatic improvements in calculation speed. Such studies are unremarkable but important because glassy systems are ubiquitous in daily life.

[1] J. A. Mydosh, *Spin Glasses: An Experimental Introduction* (Taylor and Francis, London, 1993).

[2] P. Young, *Spin Glass and Random fields* (World Scientific, Singapore, 1998).

[3] M. Henkel, M. Pleiming, and R. Sanctuary, *Aging and the Glass Transition*, 7th ed. (Springer, New York, 2007).

[4] M. Takahashi, S. Yoshimi, K.-i. Ohshima, and Y. Watanabe, Phys. Rev. B **61**, 3528 (2000).

[5] G. Ehlers, J. E. Greedan, J. R. Stewart, K. C. Rule, P. Fouquet, A. L. Cornelius, C. Adriano, P. G. Pagliuso, Y. Qiu, and J. S. Gardner, Phys. Rev. B **81**, 224405 (2010).

[6] A. G. Schins, A. F. M. Arts, and H. W. de Wijn, Phys. Rev. Lett. **70**, 2340 (1993).

[7] H. Mamiya, S. Nimori, M. Ohnuma, I. Nakatani, M. Demura, and T. Furubayashi, J. Magn. Magn. Mater. **316**, e535 (2007).

[8] H. Mamiya and S. Nimori, J. Phys.: Condens. Matter **24**, 336006 (2012).

[9] K. Jonason, E. Vincent, J. Hammann, J. P. Bouchaud, and P. Nordblad, Phys. Rev. Lett. **81**, 3243 (1998).

[10] H. Mamiya, I. Nakatani, and T. Furubayashi, Phys. Rev. Lett. **82**, 4332 (1999).

[11] M. Sasaki and K. Nemoto, J. Phys. Soc. Jpn. **69**, 2283 (2000).

[12] J. P. Bouchaud, V. Dupuis, J. Hammann, and E. Vincent, Phys. Rev. B **65**, 024439 (2001).

[13] H. Yoshino, A. Lemaître, and J. P. Bouchaud, Eur. Phys. J. B **20**, 367 (2001).

[14] P. E. Jönsson, R. Mathieu, P. Nordblad, H. Yoshino, H. A. Katori, and A. Ito, Phys. Rev. B **70**, 174402 (2004).

[15] V. Dupuis, F. Bert, J.-P. Bouchaud, J. Hammann, F. Ladieu, D. Parker, and E. Vincent, Pramana-J. Phys. **64**, 1109 (2005).

[16] H. Mamiya and S. Nimori, New J. Phys. **12**, 083007 (2010).

[17] R. Mathieu, M. Hudl, and P. Nordblad, Europhys. Lett. **90**, 67003 (2010).
[18] R. Mathieu, M. Hudl, P. Nordblad, Y. Tokunaga, Y. Kaneko, Y. Tokura, H. A. Katori, and A. Ito, Philos. Mag. Lett. **90**, 723 (2010).
[19] H. Mamiya and S. Nimori, J. Appl. Phys. **111**, 07E147 (2012).
[20] J. Villain, Z. Phys. B **33**, 31 (1979).
[21] J. N. Reimers, J. E. Greedan, R. K. Kremer, E. Gmelin, and M. A. Subramanian, Phys. Rev. B **43**, 3387 (1991).
[22] H. Mamiya, M. Onoda, T. Furubayashi, J. Tang, and I. Nakatani, J. Appl. Phys. **81**, 5289 (1997).
[23] A. S. Wills, V. Dupuis, E. Vincent, J. Hammann, and R. Calemczuk, Phys. Rev. B **62**, R9264 (2000).
[24] D. K. Singh and Y. S. Lee, Phys. Rev. Lett. **109**, 247201 (2012).
[25] A. D. LaForge, S. H. Pulido, R. J. Cava, B. C. Chan, and A. P. Ramirez, Phys. Rev. Lett. **110**, 017203 (2013).
[26] V. Dupuis, E. Vincent, J. Hammann, J.E. Greedan, and A. S. Wills, J. Appl. Phys. **91**, 8384 (2002).
[27] M. A. Hakim, M. Manjurul Haque, M. Huq, and P. Nordblad, Physica B **406**, 48 (2011).
[28] K. Kamazawa, Y. Tsunoda, H. Kadowaki, and K. Kohn, Phys. Rev. B **68**, 024412 (2003).
[29] T. Usa, K. Kamazawa, H. Sekiya, S. Nakamura, Y. Tsunoda, K. Kohn, and M. Tanaka, J. Phys. Soc. Jpn. **73**, 2834 (2004).
[30] K. Tomiyasu and K. Kamazawa, J. Phys. Soc. Jpn. **80**, SB024 (2011).
[31] H. Mamiya, I. Nakatani, and T. Furubayashi, Phys. Rev. Lett. **80**, 177 (1998).
[32] T. Jonsson, K. Jonason, and P. Nordblad, Phys. Rev. B **59**, 9402 (1999).
[33] E. Vincent, *Lecture Notes in Physics* (Springer, Berlin, 2007), Vol. 716, pp. 7–60, arXiv:cond-mat/0603583.
[34] H. W. Sheng, W. K. Luo, F. M. Alamgir, J. M. Bai, and E. Ma, Nature (London) **439**, 419 (2006).
[35] A. Zorko, O. Adamopoulos, M. Komelj, D. Arcon, and A. Lappas, Nat. Commun. **5**, 3222 (2014).
[36] F. Mezei, G. Ehlers, C. Pappas, M. Russina, T. J. Hicks, and M. F. Ling, Physica B **276–278**, 543 (2000).
[37] L. Bellier-Castella, M. J. P. Gingras, P. C. W. Holdsworth, and R. Moessner, Can. J. Phys. **79**, 1365 (2001).
[38] V. Dupuis, E. Vincent, M. Alba, and J. Hammann, Eur. Phys. J. B **29**, 19 (2002).
[39] V. Mueller and Ya. Shchur, Europhys. Lett. **65**, 137 (2004).